

Supporting Information

From 1D Nanotube Array to 2D Nanosheet Network on Silver-Coated Textile: New Insights into the Factors Determining the Performance of Core-shell Hierarchical Structure for Wearable Supercapacitors

Kaidi Li^{a, †}, Tao Zhao^{a, †}, Huifeng Wang^{b, †}, Sen Zhang^{b, *} and Chao Deng^{a, *}

^aKey Laboratory for Photonic and Electronic Bandgap Materials, Ministry of Education; Key Laboratory of Photochemical Biomaterials and Energy Storage Materials, Heilongjiang Province; Harbin Normal University, Harbin, 150025, Heilongjiang, China.

^bKey Laboratory of Superlight Material and Surface Technology, Ministry of Education; College of Material Science and Chemical Engineering, Harbin Engineering University, Harbin, 150001, Heilongjiang, China.

† Dual contributors

***Corresponding Author**

E-Mail: chaodenghsd@sina.com (C. Deng); senzhang@hrbeu.edu.cn (S. Zhang)

S-1: Experimental details

S-1-1: Synthesis of silver-coated textile

A simple electroless plating process was employed for the preparation of silver-coating layer on the textile. Firstly, the pretreatments of the textile, including precleaning, sensitizing and activating processes were carried out. The textile (2×4 cm) cut from a commercialized T-shirt was cleaned by detergent and rinsed with DI water. Then the surface sensitized process was employed by putting the cleaned textile into the sensitization solution of $\text{SnCl}_2 \cdot \text{H}_2\text{O}$ and HCl with slow stirring for 15 minutes at room temperature. The sensitized textile was rinsed in DI water for three times, followed by the activated process. The mixed solution of PdCl_2 and HCl was used as activation solution where the sensitized textile was immersed for 10 minutes. Then activated textile was further rinsed with DI water and dried under vacuum. Next, the silver-coating was prepared by a electroless deposition process. Firstly, the solution of NaOH was dropped into the AgNO_3 solution until the pH value of the mixture turns to 12~13. Then ammonia solution was dropped into the mixture until it turns to clear again, and the resultant solution is denoted as solution A. Meanwhile, $\text{C}_6\text{H}_{12}\text{O}_6$ was dissolved into DI water to form the solution B. The pretreated textile was put into solution B, and then solution A was slowly added into solution B. The silver-coating was formed by the autocatalytic reaction. Finally, the silver modified textile was washed with DI water and ethanol several times and dried under vacuum.

S-1-2: Constructing “shell-core” hierarchical electrodes based on silver-coated textile and various nanostructured materials

a) 2D nanosheets network based hierarchical structure

All the “shell-core” hierarchical electrodes were prepared based on the silver-coated textile (SCT). For the preparation of $\text{Ni}(\text{OH})_2$ nanosheets on the substrate, a simple hydrothermal method is employed. All the reagents were used as purchased with purification. Firstly, the $\text{NiCl}_2 \cdot 6\text{H}_2\text{O}$ and HMT (hexamethylenetetramine) were dissolved in 30 mL distilled water to form a transport solution. And a piece of textile substrate was placed in a filter flask. Then the mixed solution was added into the filter

flask under vacuum to let the solution wet the substrate. After the substrate was fully wetted, all of the solution and the textile was transferred into a Teflon-lined stainless steel autoclave, which was then heated at 100 °C for 5 h. The resultant Ni(OH)₂ nanosheets/SCT hierarchical electrode was then washed using distilled water and alcohol several times and dried in an oven at 80 °C.

For the preparation of NiCo-LDH nanosheets on the substrate, a simple hydrothermal strategy was employed. Firstly, the Ni(NO₃)₂·6H₂O, Co(NO₃)₂·6H₂O and HMT (hexamethylenetetramine) were dissolved in 30 mL distilled water to form a transport solution (The ration of Ni: Co is 2:1). Then the mixed solution was added into the filter flask, where a piece of SCT substrate was placed, under vacuum to let the solution wet the substrate. After the substrate was fully wetted, all of the solution and the textile was transferred into a Teflon-lined stainless steel autoclave, which was then heated at 80 °C for 8 h. The resultant NiCo-LDH nanosheets/SCT hierarchical electrode was then washed using distilled water and alcohol several times and dried in an oven at 80 °C.

b) 1D nanorods array based hierarchical structure

For the preparation of NiCo-LDH nanosheets on the substrate, the Ni(NO₃)₂·6H₂O, Co(NO₃)₂·6H₂O and urea were dissolved in 30 mL distilled water to form a transport solution (The ration of Ni: Co is 1:2). Then the mixed solution was added into the filter flask, where a piece of SCT substrate was placed, under vacuum to let the solution wet the substrate. After the substrate was fully wetted, all of the solution and the textile was transferred into a Teflon-lined stainless steel autoclave, which was then heated at 80 °C for 8 h. The resultant NiCo-LDH nanosheets/SCT hierarchical electrode was then washed using distilled water and alcohol several times and dried in an oven at 80 °C.

For the preparation of hydrate NiMoO₄ nanorods on the substrate, the Ni(NO₃)₂·6H₂O, NaMoO₄·2H₂O were used as starting materials. Firstly, NaMoO₄·2H₂O and Ni(NO₃)₂·6H₂O were dissolved in distilled water to form solution A and B. A piece of SCT substrate was placed into solution A and the solution B was added into solution A slowly. The mixed solution was refluxed under at 80 °C for 8 h. The resultant product was then washed using distilled water and alcohol several times and dried in an oven at

80 °C.

c) Central hollow nanotubes array based hierarchical structure

For the preparation of NiCo₂S₄ nanotubes on the substrate, two-steps hydrothermal treatments were employed. Firstly, the Ni(NO₃)₂·6H₂O, Co(NO₃)₂·6H₂O, NH₄F and urea were dissolved in 30 mL distilled water to form a transport solution. The mixed solution was added into the filter flask, where a piece of SCT substrate was placed under vacuum to let the solution wet the substrate. After the substrate was fully wetted, all of the solution and the textile were transferred into a Teflon-lined stainless steel autoclave, which was then heated at 120 °C for 24 h. The resultant product was then washed using distilled water and alcohol several times. Next, the resultant precursor was immersed in Na₂S solution and kept at 120 °C for 10 h. Then the product was washed and dried in an oven at 80 °C.

For the preparation of NiFeCo₂S₄ nanotubes on the substrate, two-steps hydrothermal treatments were employed. Firstly, the Ni(NO₃)₂·6H₂O, Fe(NO₃)₃·9H₂O, Co(NO₃)₂·6H₂O, NH₄F and urea were dissolved in 30 mL distilled water to form a transport solution. The mixed solution was added into the filter flask, where a piece of SCT substrate was placed under vacuum to let the solution wet the substrate. After the substrate was fully wetted, all of the solution and the textile were transferred into a Teflon-lined stainless steel autoclave, which was then heated at 120 °C for 24 h. The resultant product was then washed using distilled water and alcohol several times. Next, the resultant precursor was immersed in Na₂S solution and kept at 120 °C for 10 h. Then the product was washed and dried in an oven at 80 °C.

In the controlled experiments, the mass loading of the nanostructured active materials were in the range of 2.16~2.32 mg/cm².

S-1-3: Preparation of reference samples

The reference electrodes were prepared by same processes as described in *SI S-1-2*. The only difference is the replacement of silver-coated textile by the pristine textile to act as substrate in the synthesis process. As a result, the “shell-core” hierarchical structures are constructed by the pristine textile and different nanostructured active materials.

S-2: Materials characterizations

Powder X-ray diffraction (XRD, Bruker D8/Germany) using Cu K α radiation was employed to identify the crystalline phase of the material. The experiment was performed by using step mode with a fixed time of 3 s and a step size of 0.02°. The XRD pattern was refined by using the Rietveld method. The morphology was observed with a scanning electron microscope (SEM, HITACHIS-4700) and a transmission electron microscope (TEM, JEOS-2010 PHILIPS). The element distribution of the sample was confirmed by energy dispersive X-ray detector (EDX). Nitrogen adsorption-desorption isotherms were measured using a Micromeritics ASAP 2010 sorptometer and specific surface area were calculated correspondingly. The electronic conductivities of all the samples are measured using the four-point probe method (LORESTA GP, MCP-T610).

S-3: Electrochemical measurements

The prepared hierarchical electrodes are directly used as electrode without additional components such as binder, conductive additive or current collector. The electrochemical performance of the single electrode is tested in the three-electrode system, where the hierarchical electrodes are used as working electrode, the Pt foil is used as the counter electrode and the Ag/AgCl electrode is used as reference electrode. The KOH solution was used as electrolyte. All-solid-state capacitors were assembled by the hierarchical electrode as positive electrode, the RGO film as negative electrode and electrolyte poly(vinyl alcohol) (PVA)/KOH as the separator and electrolyte. Solid gel electrolyte was prepared by dissolving KOH and PVA powder into DI water, which was firstly slowly stirred for 2 hours at room temperatures and then heated to 95 °C until it became clear. The resultant solution was mold to achieve a PVA/KOH gel membrane. In both systems, the cyclic voltammetry (CV) and electrochemical impedance (EIS) were measured in a Zivlab electrochemical workstation, and the galvanostatic charge/discharge tests were conducted on a LAND battery testing system (Wuhan, China).

S-4: Description of the electrochemical performance of single electrode

The performance of the single electrode are described by the follow equations,

(1) specific capacitance (SC)

The specific capacitance of the single electrode is calculated based on the galvanostatic charge/discharge curves,

$$SC = \frac{I \times \Delta t}{m \times \Delta V} \quad (1)$$

Where SC is the specific capacitance, Δt is the discharge time, I is the discharge current, ΔV is the voltage change of discharge, m is the mass of the active material in the single electrode.

(2) Cycling retention (CR)

The cycling retention of the single electrode is calculated based on the following equation,

$$CR = \frac{Q_{sc}(after)}{Q_{sc}(before)} \quad (2)$$

Where CR is the capacitance retentions after cycling, Q_{sc} (after) is the specific capacitance of the electrode after cycling, Q_{sc} (before) is the specific capacitance of the electrode before cycling,

(3) Relative capacitance (SC_r)

The relative capacitance of the single electrode is calculated based on the following equation,

$$SC_r = \frac{SC(i)}{SC(0.5)} \quad (3)$$

Where SC is the relative capacitance, $SC(i)$ is the specific capacitance at a certain current density, $SC(0.5)$ is the specific capacitance at 0.5 A g^{-1} .

(4) The ratios of electrochemical resistance before and after cycling (R_r)

$$R_r = \frac{R(after)}{R(before)} \quad (4)$$

Where R_r is the ratios of the electrochemical resistance; R (after) is the electrochemical resistance (R_s and R_{ct}) after cycling; R (before) is the electrochemical resistance (R_s and R_{ct}) before cycling.

S-5: Description of the electrochemical performance of asymmetric supercapacitors

(1) specific capacitance (*SC*)

The specific capacitance of the supercapacitor is calculated based on the galvanostatic charge/discharge curves,

$$SC = \frac{I \times \Delta t}{m \times \Delta V} \quad (5)$$

Where *SC* is the specific capacitance, Δt is the discharge time, *I* is the discharge current, ΔV is the voltage change of discharge, *m* is the mass of the active materials in both positive and negative electrodes.

(2) Energy density (*E*) and power density (*P*)

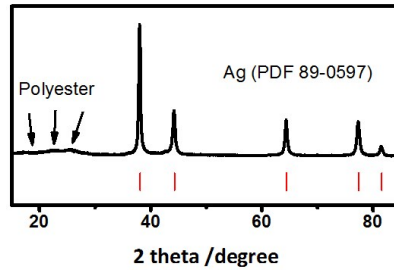
$$E = 0.5 \times C \times \Delta V^2 \quad (6)$$

$$P = \frac{E}{\Delta t} \quad (7)$$

Where *E* is the energy density, *P* is the power density, *C* is the specific capacitance, Δt is the discharge time, ΔV is voltage change of discharge.

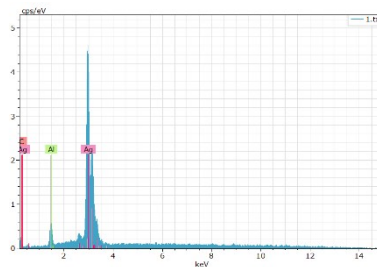
S-6: Supporting figures

Figure S-1



XRD pattern of the silver-coated textile is in good agreement of the standard spectroscopy of Ag, which demonstrates the presence of silver-coating on the textile.

Figure S-2



EDS results of the silver-coated textile demonstrate the presence of silver elements on the textile. The element of Al is the base for the samples in the EDS testing.

Figure S-3

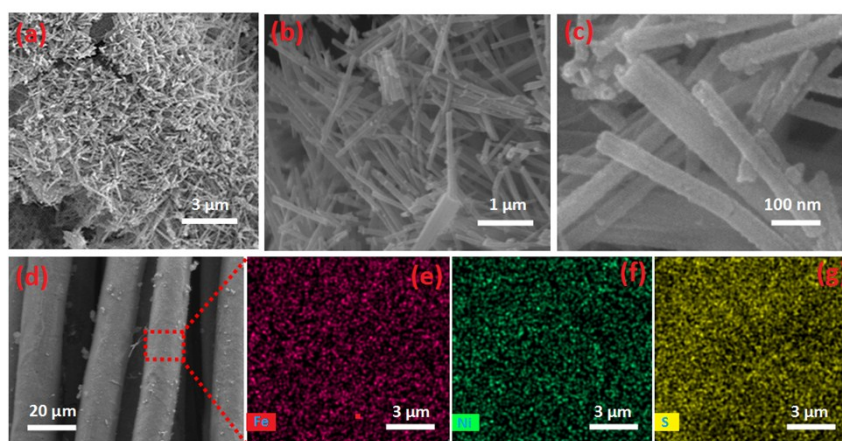
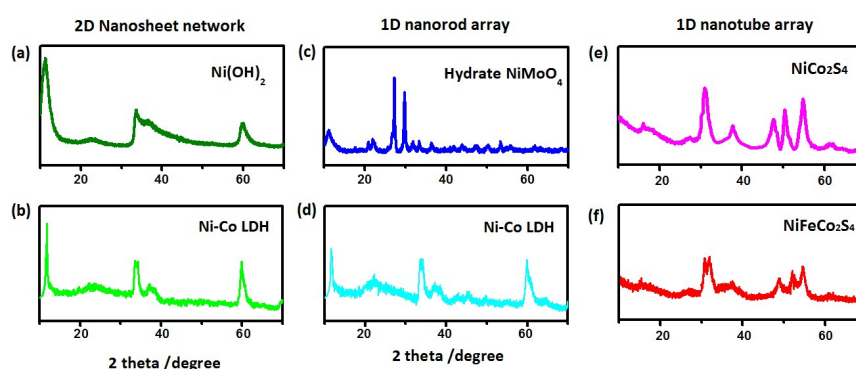


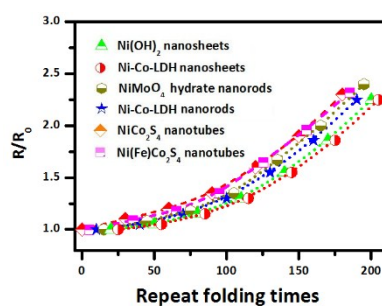
Figure S-3 (a~d) Morphology and (e~f) EDX element mapping (Fe, Ni and S) of NiFeCo₂S₄ nanotubes. SEM images (a~d) indicate the prepared NiFeCo₂S₄ has central hollow nanotubes with microscale length (1~2 μm), uniform diameter (50~100 nm) and ultrathin shell thickness (~10 nm). The elements distributions in EDX results (e~f) demonstrate the uniform distributions of the Fe (red), Ni (green) and S (yellow) elements along with the whole fiber.

Figure S-4



XRD patterns of the Ni(OH)₂ (a) and Ni-Co LDH (b) nanosheet, NiMoO₄ hydrate and Ni-Co LDH (b) nanorods, and NiCo₂S₄ and NiFeCo₂S₄ nanotubes.

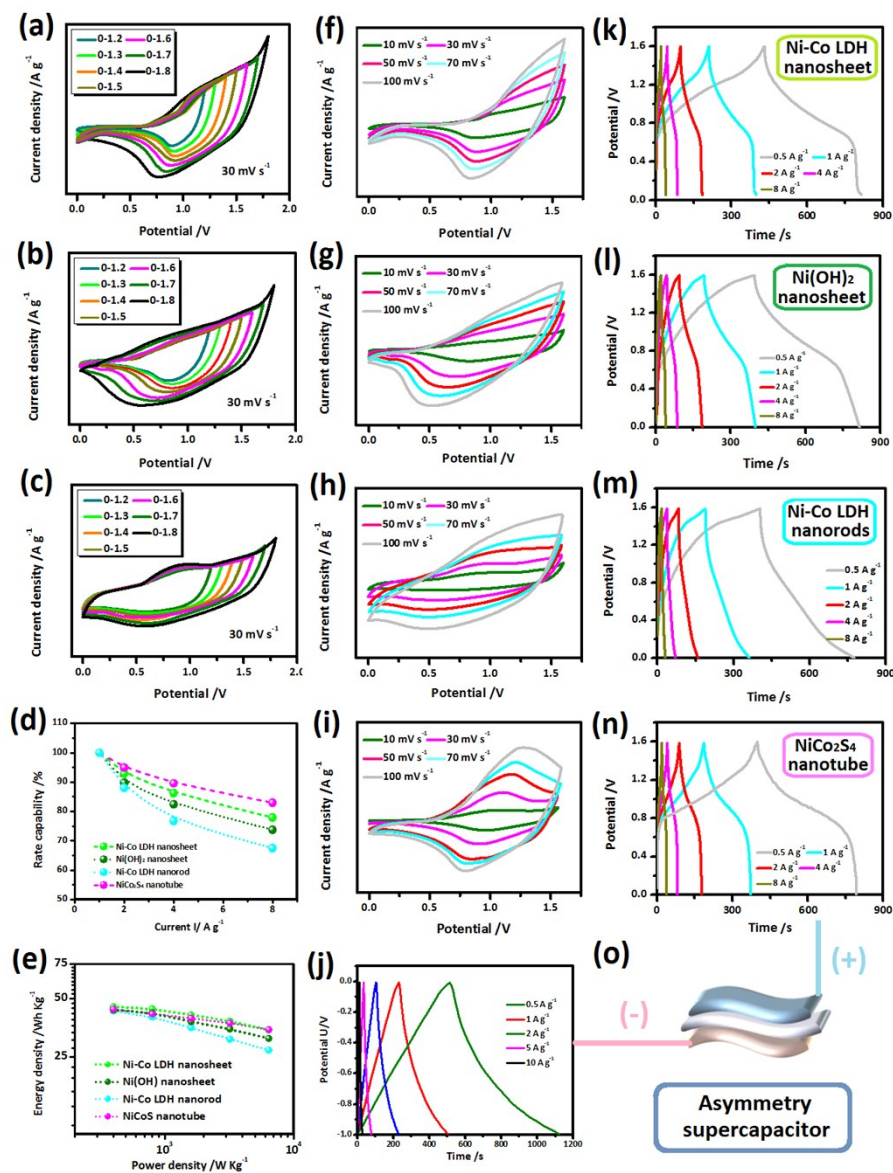
Figure S-5



The quick resistance enhancements are observed for the reference samples based on the pristine

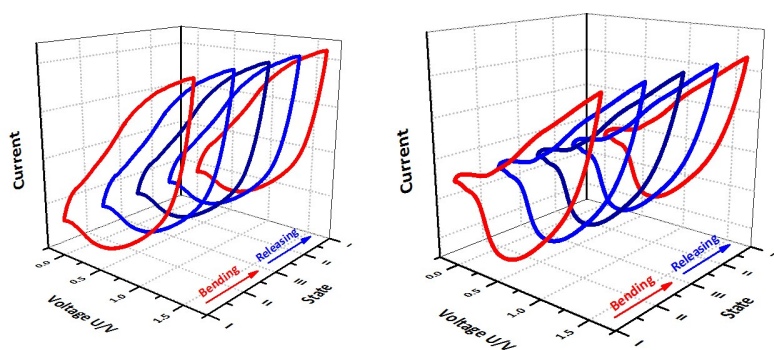
textile during repeated folding demonstrate their inferior structure stability.

Figure S-6



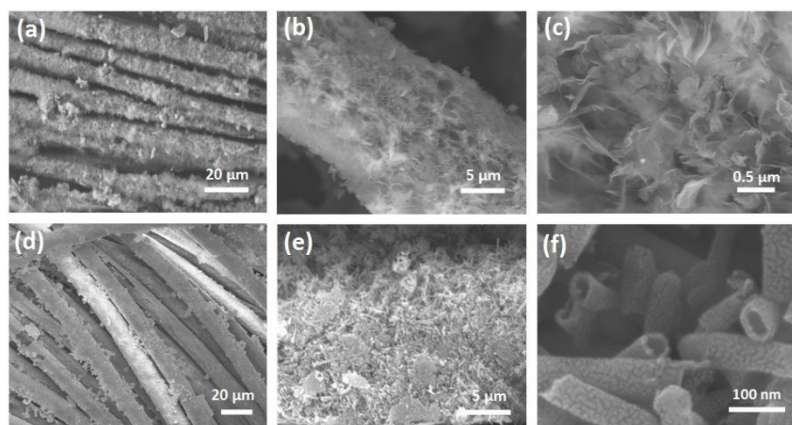
Schematic illustration (o) of asymmetry supercapacitors based on the positive electrode of Ni-Co-LDH nanosheet (a, f, k), Ni(OH)₂ nanosheet (b, g, l), Ni-Co-LDH nanorod (c, h, m) and NiCo₂S₄ nanotube (i, n) and negative electrode of RGO (j). (a~c) CV curves of the capacitors at different voltage range. (f~i) CV curves and (k~n) galvanostatic charge/discharge curves of the capacitors at various scan rates or current densities. (d) Rate capabilities and (e) Ragone plot of the capacitors.

Figure S-7



CV curves of the capacitors with Ni(OH)₂ nanosheet network (right) and Ni-Co LDH nanorod (left) based electrodes in different degree of bending (from state I to III) and releasing (from state III to I).

Figure S-8



Morphology of cycled electrodes based on silver-coated textile substrate and NiCo-LDH nanosheets (a~c) and NiCo₂S₄ nanotubes (d~f). The architectures of both hierarchical electrodes are maintained after long-term charge/discharge cycling, demonstrating their good structure stability.

S-7: Supporting tables

Table S-1 Comparisons of the capacitance and cycling stability of the electrode materials including Ni(OH)₂ (a), NiCo-LDH (b), NiMoO₄ (c), NiCo₂S₄ (d) and NiFeCo₂S₄ (e) in our work and the relative results reported by other groups.

Materials	morphology	Specific capacitance	Cycling retention	References
(a) Ni(OH) ₂	Flower-like nanospheres composed of nanowires	1610.8 F g ⁻¹ (1 A g ⁻¹)	700 cycles 96%	1
(a) Ni(OH) ₂	Nanoporous thin film on 3D graphite foam	1610.8 F g ⁻¹ (0.5 A g ⁻¹)	400 cycles 65%	2

(a) Ni(OH) ₂	3D nanoporous thin film	1500 F g ⁻¹ (1 A g ⁻¹)	5000 cycles 90%	3
(a) Ni(OH) ₂	Nanocrystals on graphene sheet	1335 F g ⁻¹ (2.8 A g ⁻¹)	2000 cycles 100%	4
(a) Ni(OH) ₂ (sample b)	“shell-core” hierarchical structure with nanosheets type shells	1765 F g ⁻¹ (1 A g ⁻¹)	5000 cycles 89.5%	This work

Materials	morphology	Specific capacitance	Cycling retention	References
(b) NiCo-LDH	Nanorod on CNF	1378.2 F g ⁻¹ (1 A g ⁻¹)	1000 cycles 60.3%	5
(b) NiCo-LDH	Nanosheet on CNF	1195.4 F g ⁻¹ (1 A g ⁻¹)	1000 cycles 61%	5
(b) NiCo-LDH	Nanosheet on biomass derived N-doped carbon nanofiber	1949.5 F g ⁻¹ (1 A g ⁻¹)	5000 cycles 74.4%	6
(b) NiCo-LDH	Nanosheet on Nickel Foam	2435 F g ⁻¹ (6 A g ⁻¹)	5000 cycles 82%	7
(b) NiCo-LDH (sample a)	“shell-core” hierarchical structure with nanosheets type shells	2218 F g ⁻¹ (0.5 A g ⁻¹)	5000 cycles 92.8%	This work
(b) NiCo-LDH (sample d)	“shell-core” hierarchical structure with nanorod type shells	2009 F g ⁻¹ (0.5 A g ⁻¹)	5000 cycles 86.6%	This work

Materials	morphology	Specific capacitance	Cycling retention	References
(c) NiMoO ₄ hydrate	1D Nanorod	312 F g ⁻¹ (5 A g ⁻¹)	1000 cycles 77%	8
(c) NiMoO ₄ hydrate (sample c)	“shell-core” hierarchical structure with nanorod type shells	1167 F g ⁻¹ (0.5 A g ⁻¹)	5000 cycles 84%	This work

Materials	morphology	Specific capacitance	Cycling retention	References
(d) NiCo ₂ S ₄	Nanotube on Ni foam	783 F g ⁻¹ (2 A g ⁻¹)	4000 cycles 93.4%	9
(d) NiCo ₂ S ₄	Nanosheet on Ni foam	1231 F g ⁻¹ (2 A g ⁻¹)	2000 cycles 90.4%	10
(d) NiCo ₂ S ₄	Hierarchical nanotube@nanosheet arrays on Ni foam	1460 F g ⁻¹ (1 A g ⁻¹)	4500 cycles 87.5%	11

(d) NiCo ₂ S ₄	NiCo ₂ S ₄ @MnO ₂ heterostructures	1337.8 F g ⁻¹ (2 A g ⁻¹)	2000 cycles 82%	12
(d) NiCo ₂ S ₄ (sample e)	“shell-core” hierarchical structure with nanotube type shells	1965 F g ⁻¹ (0.5 A g ⁻¹)	5000 cycles 90.2%	This work
Materials	morphology	Specific capacitance	Cycling retention	References
(e) NiFeCo ₂ S ₄	Nanotube on Silver-sputtered textile	1518.5 F g ⁻¹ (5 mA cm ⁻²)	Not mentioned	13
(e) FeCo ₂ S ₄	Nanosheet on Ni foam	2411 F g ⁻¹ (5 mA cm ⁻²)	5000 cycles 92%	14
(e) NiFeCo ₂ S ₄ (sample f)	“shell-core” hierarchical structure with nanotube type shells	2185 F g ⁻¹ (0.5 A g ⁻¹)	5000 cycles 92%	This work

References for Table S-1

- [1] H. M. Du, L. F. Jiao, K. Z. Cao, Y. J. Wang, H. T. Yuan, *ACS Appl. Mater. Interfaces* 2013, 5, 6643-6648.
- [2] J. Y. Ji, L. L. Zhang, H. X. Ji, Y. Li, X. Zhao, X. Bai, X. B. Fan, F. B. Zhang, R. S. Ruoff, *ACS Nano*, 2013, 7, 6237-6243.
- [3] Y. Yang, L. Li, G. D. Ruan, H. L. Fei, C. S. Xiang, X. J. Fan, J. M. Tour, *ACS Nano* 2014, 8, 9622-9628.
- [4] H. L. Wang, H. S. Casalongue, Y. Y. Liang, H. J. Dai, *J. Am. Chem. Soc.* 2010, 132, 7472-7477.
- [5] F. L. Lai, Y. P. Huang, Y. E. Miao, T. X. Liu, *Electrochimica Acta* 2015, 174, 456-463.
- [6] F. L. Lai, Y. E. Miao, L. Z. Zuo, H. Y. Lu, Y. P. Huang, T. X. Huan, *Small* 2016, 12, 3235-3244.
- [7] H. Chen, L. F. Hu, M. Chen, Y. Yan, L. M. Wu, *Adv. Funct. Mater.* 2014, 24, 934-942.
- [8] D. Ghosh, S. Giri, C. K. Das, *Nanoscale*, 2013, 5, 10428-10437.
- [9] J. Pu, T. T. Wang, H. Y. Wang, Y. Tong, C. C. Lu, W. Kong, Z. H. Wang, *ChemPlusChem* 2014, 79, 577-583.
- [10] L. F. Shen, J. Wang, G. Y. Xu, H. S. Li, H. Dou, X. G. Zhang, *Adv. Energy Mater.* 2014, 1400977.
- [11] H. C. Chen, S. Chen, H. Y. Shao, C. Li, M. Q. Fan, D. Chen, G. Tian, K. Y. Shu, *Chem. Asian J.* 2016, 11, 248-255.
- [12] J. Yang, M. Ma, C. C. Sun, Y. F. Zhang, W. Huang, X. C. Dong, *J. Mater. Chem. A* 2015, 3, 1258-1264.
- [13] J. Zhu, S. C. Tang, J. Wu, X. L. Shi, B. G. Zhu, X. K. Meng, *Adv. Energy Mater.* 2016, 1601234.
- [14] S. C. Tang, B. G. Zhu, X. L. Shi, J. Wu, X. K. Meng, *Adv. Energy Mater.* 2017, 7, 1601985.